The ISME Journal (2017), 1–11

www.nature.com/ismej

ORIGINAL ARTICLE

Soil microorganisms can overcome respiration inhibition by coupling intra- and extracellular metabolism: ^{13}C metabolic tracing reveals the mechanisms

Ezekiel K Bore[1], Carolin Apostel[1,2], Sara Halicki[1], Yakov Kuzyakov[1,2] and Michaela A Dippold[1]

[1]*Department of Agricultural Soil Science, Georg-August-University Goettingen, Goettingen, Germany and* [2]*Soil Science of Temperate Ecosystems, Georg-August-University Goettingen, Goettingen, Germany*

CO_2 release from soil is commonly used to estimate toxicity of various substances on microorganisms. However, the mechanisms underlying persistent CO_2 release from soil exposed to toxicants inhibiting microbial respiration, for example, sodium azide (NaN_3) or heavy metals (Cd, Hg, Cu), remain unclear. To unravel these mechanisms, NaN_3-amended soil was incubated with position-specifically ^{13}C-labeled glucose and ^{13}C was quantified in CO_2, bulk soil, microbial biomass and phospholipid fatty acids (PLFAs). High ^{13}C recovery from C-1 in CO_2 indicates that glucose was predominantly metabolized via the pentose phosphate pathway irrespective of inhibition. Although NaN_3 prevented ^{13}C incorporation into PLFA and decreased total CO_2 release, ^{13}C in CO_2 increased by 12% compared with control soils due to an increased use of glucose for energy production. The allocation of glucose-derived carbon towards extracellular compounds, demonstrated by a fivefold higher ^{13}C recovery in bulk soil than in microbial biomass, suggests the synthesis of redox active substances for extracellular disposal of electrons to bypass inhibited electron transport chains within the cells. PLFA content doubled within 10 days of inhibition, demonstrating recovery of the microbial community. This growth was largely based on recycling of cost-intensive biomass compounds, for example, alkyl chains, from microbial necromass. The bypass of intracellular toxicity by extracellular electron transport permits the fast recovery of the microbial community. Such efficient strategies to overcome exposure to respiration-inhibiting toxicants may be exclusive to habitats containing redox-sensitive substances. Therefore, the toxic effects of respiration inhibitors on microorganisms are much less intensive in soils than in pure cultures.

The ISME Journal advance online publication, 3 February 2017; doi:10.1038/ismej.2017.3

Introduction

Soil microbes are the primary drivers of soil organic matter (SOM) cycling. However, microbial activity can be altered by human activities such as fertilization, use of pesticides or soil contamination by heavy metals from mines, industrial, agricultural and technological application. The rate and amount of CO_2 evolved from soil are used to evaluate the effects of toxicants (for example, heavy metals and other pollutants) on heterotrophic microorganism activity in SOM decomposition (Babich and Stotzky, 1985; ISO 16072). Persistent CO_2 release from soils exposed to toxicants (Voroney and Paul, 1984; Trevors, 1996) or contaminated with heavy metals (Bond *et al.*, 1976; Ausmus *et al.*, 1978; Fliessbach *et al.*, 1994) remains unclear. Understanding the mechanisms responsible for CO_2 emission under such disturbances is important for predicting the response of nutrient and C cycles to future anthropogenic environmental changes (Schimel, 2013). Knowledge of metabolic pathways through which organic substances are oxidized to CO_2 is crucial in unraveling these mechanisms, making metabolic tracing an invaluable tool for identifying alterations in microbial transformation pathways of organic substances under these unfavorable conditions (Scandellari *et al.*, 2009; Dijkstra *et al.*, 2011a; Dippold *et al.*, 2014).

Microorganisms break down complex plant materials such as cellulose to produce easily available water-soluble substances such as glucose, the most abundant monomer in soil, from which about 60–70% is incorporated into cellular compounds while 30–40% is oxidized for energy (Fischer *et al.*, 2007; Gunina and Kuzyakov, 2015). Sufficient amounts of glucose in soil solution can activate microbial metabolism and induce growth (Blagodatskaya and Kuzyakov, 2013; Mau *et al.*, 2015),

Correspondence: EK Bore, Department of Agricultural Soil Science, Georg-August University of Goettingen, Buesgenweg 2, 37077 Goettingen, Lower Saxony, Germany.
E-mail: ezekielbore7@gmail.com
Received 29 May 2016; revised 24 November 2016; accepted 4 January 2017

hence accelerating SOM decomposition. In sterile soil, approximately 98% of glucose remains K_2SO_4-extractable within 24 h (Bremer and van Kessel, 1990). Glucose lacks physical or chemical interactions with soil due to an absence of charged functional groups or hydrophobic parts (Fischer *et al.*, 2010; Apostel *et al.*, 2015), making it a potent candidate for tracing soil metabolic processes. Furthermore, the use of position-specifically labeled glucose allows the fate of individual molecular positions to be determined (Scandellari *et al.*, 2009; Dijkstra *et al.*, 2011a; Apostel *et al.*, 2015), permitting detailed reconstruction of microbial metabolic pathways and *de novo* formed products (Dippold and Kuzyakov, 2013). This provides the toolbox required to elucidate the source of CO_2 emission under respiration-inhibited conditions and thus to identify the mechanisms to overcome intoxication in contaminated environments.

In this study, microbial respiration was inhibited via NaN_3 addition, a potent electron transport chain inhibitor at cytochrome oxidase and catalase (Keilin, 1936), resulting in cell asphyxiation (Winter *et al.*, 2012). Paradoxically, azide addition increases CO_2 efflux from soil (Rozycki and Bartha, 1981; Trevors, 1996). This cannot be attributed to errors in CO_2 determination caused by formation of volatile hydrazoic (HN_3) acid (Rozycki and Bartha, 1981; Trevors, 1996), as chloroform fumigation also results in persistent CO_2 emission (Voroney and Paul, 1984; Blankinship *et al.*, 2014). The CO_2 emitted from soil following microbial metabolic inhibition was previously ascribed to active oxidative extracellular enzymes (EXOMET) already present in soil or released from dead cells (Maire *et al.*, 2013). However, since this study solely traced catabolism, the ultimate source of the emitted CO_2 could not be definitively concluded.

This study aimed to establish the origin and underlying mechanisms of persistent CO_2 release from soils exposed to model toxicants inhibiting respiratory chains. Analysis of position-specific ^{13}C patterns in CO_2, soil, microbial biomass and phospholipid-derived fatty acid (PLFA) was performed to elucidate mechanisms underlying inhibition-induced CO_2 release. Measuring the production of *de novo* formed microbial compounds was used as criteria to confirm or reject existence of intracellular metabolism following inhibition. Production of PLFAs, components of microbial cell membranes only formed by intact and proliferating cells, is frequently utilized to confirm the presence of active intracellular metabolism. We hypothesized that a lack of ^{13}C incorporation from labeled glucose into microbial biomass and PLFA after inhibition would confirm the proposed EXOMET theory.

Materials and methods

Sampling site

The soil was sampled from agriculturally used loamy Luvisol in northern Bavaria (49°54′ northern latitude; 11°08′ eastern longitude, 500 a.s.l.) with a mean annual temperature of 7 °C, and a mean annual precipitation of 874 mm. The soil had a pH (KCl) of 4.88, a pH (H_2O) of 6.49, a TOC and TN content of 1.77% and 0.19%, respectively. Cation exchange capacity was 13 $cmol_C\ kg^{-1}$. The soil was collected from 0–10 cm, air dried, sieved to 2 mm and stored at 5 °C until use.

Experimental design

Incubations were conducted in screw-cap glass microcosms with a base layer of quartz sand. Eighty grams of dry soil was transferred to soil sample rings and installed on ceramic plates above the quartz sand. Half of the rings received NaN_3 to inhibit microbial activity while the second set was not treated with NaN_3 (Control). The 10 ml of 2 mM NaN_3 solution added to each ring was subdivided into two portions: (1) 2 ml was added directly onto the soil surface and (2) 8 ml to the sand (to be taken up through the ceramic plates) while control soils received 10 ml of water. The added volume of water rewetted the soil to field capacity. All microcosms were preconditioned for 24 h at 5 °C. This temperature was used to eliminate interference of the CO_2 determination by volatile HN_3 formed from the conversion of NaN_3 in soil. Four position-specific ^{13}C-labeled isotopomeres of glucose (^{13}C-1, ^{13}C-2, ^{13}C-4 and ^{13}C-6), uniformly ^{13}C-labeled (U-^{13}C) and non-labeled glucose (natural abundance background) were applied to the soil in separate microcosms with four replicates each and three sampling dates resulting in 144 individual microcosms. Five milliliter of 2.55 mM glucose solution was applied onto the soil surface in each microcosm. Glucose solution for the treated soil contained 1 mM NaN_3 to maintain continued inhibition. Cups filled with 5 ml of 1 M NaOH were placed into each microcosm to trap CO_2. Microcosms were sealed and incubated at 5 °C in the dark.

Sampling and sample preparation

NaOH in the vials was sampled and replaced after 10 h, 1, 2, 3, 6 and 10 days. Soils were sampled after 1, 3 and 10 days. Each sample was divided into two fractions: 30 g of each sample was immediately subjected to chloroform-fumigation extraction as described below, while the remainder was stored at −20 °C for PLFA analysis.

Analytical methods

Amount and $\delta^{13}C$ value of CO_2. About 0.4 ml of each CO_2 trap was diluted 1:10 with ultrapure water and CO_2 content was determined by a non-dispersive infrared (NDIR) gas analyzer (TOC 5050; Shimadzu Corporation, Kyoto, Japan). The remaining volume was precipitated with 5 ml of 0.5 M $SrCl_2$ solution.

Precipitates of $SrCO_3$ were separated by fourfold centrifuging at 2000 × *g* for 10 min and washing in between with millipore water to remove NaOH until pH 7 was reached. Dried $SrCO_3$ samples (1–2 mg) were loaded into tin capsules and $\delta^{13}C$ value was measured with a Flash 2000 Elemental analyzer coupled by a ConFlo III interface to a Delta V advantage Isotope Ratio Mass Spectrometer IRMS (all units from Thermo Fisher Scientific, Bremen, Germany). ^{13}C respired from the applied glucose was calculated according to a mixing model (Equations (1) and (2)), where the C content of the background ($[C]_{BG}$) in Equation (1) was determined by Equation (2) (Gearing, 1991)

$$[C]_{CO_2} \cdot r_{CO_2} = [C]_{BG} \cdot r_{BG} + [C]_{appG} \cdot r_{appG} \quad (1)$$

$$[C]_{CO_2} = [C]_{BG} + [C]_{appG} \quad (2)$$

where $[C]_{CO_2/BG/appG}$ C content of the sample/background/applied glucose (mg C g^{-1}soil); $r_{CO_2/BG/appG}$ ^{13}C atom %-excess of labeled sample/background/applied glucose (at%).

Bulk soil C and ^{13}C content measurement. Aliquots of samples were freeze dried, ground in ball mill and 13–15 mg were weighted into tin capsules. Carbon stable isotope measurement were performed with EuroVektor elemental analyzers (HEKAtech GmbH, Wegberg, Germany) coupled by a ConFlo III interface to a Delta Plus XP IRMS (both units from Thermo Fisher Scientific). Incorporation of ^{13}C from applied glucose into soil was calculated according to Equations (1) and (2).

Microbial biomass ^{13}C determination. Microbial biomass C and $\delta^{13}C$ values were determined by chloroform fumigation extraction. Soil samples were divided into two subsets of 12 g each. One subset was extracted directly and the other subset was first fumigated with chloroform for 3 days in a desiccator to lyse microbial cells. Organic C was extracted with 36 ml of 0.05 M K_2SO_4 on an orbital shaker for 1.5 h. Samples were centrifuged for 10 min at 2000 r.p.m. and the supernatant was filtered and frozen at −20 °C until C content analysis on a TOC/TIC analyzer (Multi C/N 2100 AnalytikJena, Jena, Germany). Thereafter, the extracts were freeze dried and about 25 mg (fumigated) and 40 mg (unfumigated) were used for $\delta^{13}C$ values determination via EA-IRMS. Incorporation of ^{13}C into fumigated and unfumigated samples was calculated using Equations (1) and (2). Microbial biomass C was calculated by subtracting unfumigated from fumigated C and dividing the product by a correction factor of 0.45 (Wu *et al.*, 1990).

PLFA extraction and analysis

PLFA extraction and purification. PLFAs were analyzed according to a modified method by Frostegård *et al.* (1991) with each step described in detail in Gunina *et al.* (2014). Briefly, 25 µg of an internal recovery standard (phosphatidylcholine-dinonadecanoic acid) was added to 6 g frozen soil. PLFAs were repeatedly extracted (first with 18 ml, then with 6 ml) with a 2:1:0.8 mixture of methanol, chloroform and 0.15 M citric acid adjusted to pH 4. A two-phase mixture was generated from the combined extracts by addition of chloroform and citric acid. After shaking the lower chloroform phase was removed by liquid–liquid extraction. Neutral and glycolipids were separated from phospholipids on a solid phase extraction column packed with activated silica gel by elution with chloroform, acetone and methanol, respectively. Phospholipids were hydrolyzed in 0.5 M NaOH in methanol for 10 min on 100 °C and derivatized to fatty acid methyl esters by heating with 10% boron trifluoride in methanol at 80 °C for 15 min. Fifteen micrograms of the second external standard (tridecanoate methyl ester) together with 185 µl toluene were added to the sample and then transferred into 1.5 ml GC vials.

Analysis of $\delta^{13}C$ values on GC-C-IRMS. One microliter of PLFA samples were injected with a 1 min splitless time into a liner at 280 °C of a Trace GC coupled via a GC-C III interface to a Delta plus IRMS (all units from Thermo Fisher Scientific). Peak separation was accomplished with two capillary columns (DB1-MS, 15 m, 250 µm ID, 0.25 µm film thickness and DB-5 MS, 30 m 250 µm ID, 0.25 µm film thickness) with helium (He 99.99% pure) as carrier gas at a flow rate of 1.7 ml per min.

Fatty acid methyl esters peaks were integrated and the $\delta^{13}C$ values (‰) calculated via ISODAT 2.0. Drift correction was performed via repeated injection of the reference gas (CO_2 99.995% pure) during measurement by linear regressions between the gas peaks surrounding the sample peaks. Correction functions according to Glaser and Amelung (2002) were used to account for the unknown $\delta^{13}C$ value of the derivatization agents and concentration-dependent isotopic fractionation during the measurement (Schmitt *et al.*, 2003). PLFA-C was quantified by (1) relating each fatty acid methyl esters area to the area of IS 2, (2) calculating calibration curves by linear regression of external standards consisting of 27 fatty acids at five increasing concentrations (see Supplementary Table S1) and (3) correcting for the recovery of the initially added phospholipid standard.

Statistical analysis

A Nalimov outlier test was performed for the respiration data with significance levels of 95% in case of four replicates. Microbial grouping was done by factor analysis of relative PLFA amounts (Apostel *et al.*, 2013; Gunina *et al.*, 2014). PLFA were grouped to one microbial group if they loaded on the same factor higher than 0.5 and if literature data on pure cultures proved their common origin (Zelles, 1999; Zelles *et al.*, 1995). Incorporation of ^{13}C into bulk soil, microbial biomass, PLFAs and into CO_2 was

tested for significant differences between the positions, incubation time and effect of NaN_3 addition via factorial analysis of variance (ANOVA). If assumptions of normal distribution and homogeneous variances were not met, then outcomes were validated by a nonparametric Kruskal Wallis ANOVA. Significant differences were determined with Tukey Honest Significance Difference (Tukey HSD) *post hoc* test at a confidence level of 99.95%. Statistical tests were performed with Statistica (version 12.0; Statsoft GmbH, Hamburg, Germany).

Results

CO_2 efflux and ^{13}C recovery

Ten days after glucose application, total CO_2 respired from azide-treated soil was twofold lower compared with control (Figure 1, top left). Two stages of glucose mineralization independent of inhibition were observed: (1) high ^{13}C recovery in CO_2 within the first 3 days and (2) low ^{13}C recoveries thereafter (Figure 1, bottom). There were clear differences in ^{13}C recovery from the individual glucose positions in CO_2, especially in the first phase. Position-specific ^{13}C recovery in CO_2 followed a classical pattern characteristic of high pentose phosphate pathway activity, with C-1 > C-4 > C-2 > C-6, irrespective of inhibition. On average, ^{13}C recovery in CO_2 was 12% higher in inhibited soil compared with control (Figure 1, bottom), with the largest difference occurring within the first day (Figure 1, top right).

Glucose ^{13}C incorporation into bulk soil and microbial biomass

Azide addition resulted in alteration of the ^{13}C recovery patterns. At day 1, ^{13}C recoveries from C-2 and C-4 in inhibited bulk soil were 17% and 20% lower compared with control (Figure 2). ^{13}C recovery in bulk soil with inhibition did not differ between day 1 and 3 but decreased by over 12% at day 10 for each position, suggesting a shift in C transformations between day 3 and 10. In contrast, ^{13}C recovery in control soil did not differ between the days for each glucose position. Moreover, the ^{13}C recovery in bulk soil was five times higher than in microbial biomass, 3 days after inhibition (Figure 2), whereas in control only twice as much ^{13}C was in bulk soil than in microbial biomass after 3 days.

Position-specific patterns of ^{13}C incorporation into microbial biomass were similar irrespective of

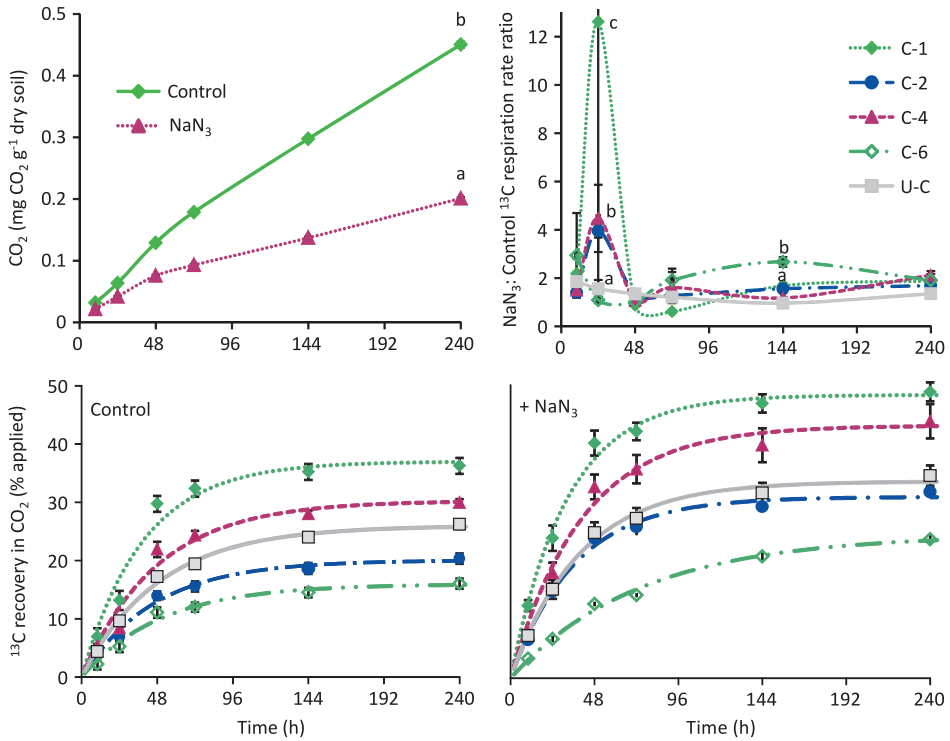

Figure 1 Cumulative CO_2 (mean ± s.e.) from ^{13}C uniformly labeled glucose respired during 10 days in control and NaN_3-treated soils (top left), +NaN_3:Control ^{13}C (mean ± s.e.) respiration rate ratio from individual glucose position (top right) and cumulative ^{13}C (mean ± s.e.) recovered in CO_2 released from position-specific ^{13}C-labeled glucose applied to soil with control (bottom left) and azide-exposed (bottom right). ^{13}C curves were fitted with nonlinear least-square regressions according to an exponential equation ($cum^{13}C(t) = {}^{13}C_{max} * (1 - e^{-kt})$), where cum ^{13}C (t) is the cumulative ^{13}C amount depending on time, $^{13}C_{max}$ is the parametrically determined maximum of ^{13}C, k is the mineralization rate and t is time (parameter estimates in Supplementary Table S4). Steven' runs test for the fitted ^{13}C curves revealed no deviation from linearity (Supplementary Table S5). Significant differences between fitted curves are displayed in Supplementary Table S6.

respiration inhibition by NaN_3. However, ^{13}C recovery was threefold lower in microbial biomass after inhibition compared with control (Figure 2).

Microbial community composition

Grouping of PLFAs resulted in 10 functional microbial groups (Supplementary Table S2). In general, the biomarkers of Gram positive 2 (G+2) were dominant followed by those of Gram negative 2 (G-2) irrespective of inhibition (Figure 3, left). At day 1, the amounts of fatty acids extracted were over twofold lower in inhibited soils compared with control (Figure 3, left). Ten days after inhibition, fatty acid contents doubled to levels similar to control and pattern of fatty acid did not differ between treatments suggesting complete recovery of the microbial community in inhibited soil.

The fungal/bacterial (Fu/Ba) ratio did not differ between the days in control soils (Figure 3, right). In azide-treated soil, however, Fu/Ba ratio increased twofold between day 1 and 3, attaining similar levels at day 3 in both treatments and remained constant till day 10 (Figure 3, right).

Glucose ^{13}C uptake by microbial groups

In control soil, ^{13}C recovery was highest in PLFAs of G-2 and G+2, with each group containing approximately 0.09% of the applied glucose ^{13}C in their membrane fatty acids. The other groups only incorporated between 0.01 and 0.04% of applied ^{13}C. Incorporation of ^{13}C into the PLFA of each microbial group did not differ between the days in both treatments (Figure 4).

In respiration-inhibited soil, however, there was no ^{13}C incorporation into microbial PLFAs within the first 3 days (Figure 4). After 10 days, less than 0.007% of applied ^{13}C was recovered in PLFAs of G +2, Actinomycetes 1 and 2 (Ac1 and Ac2; Figure 4). The other microbial groups did not incorporate measurable ^{13}C into PLFAs 10 days after azide

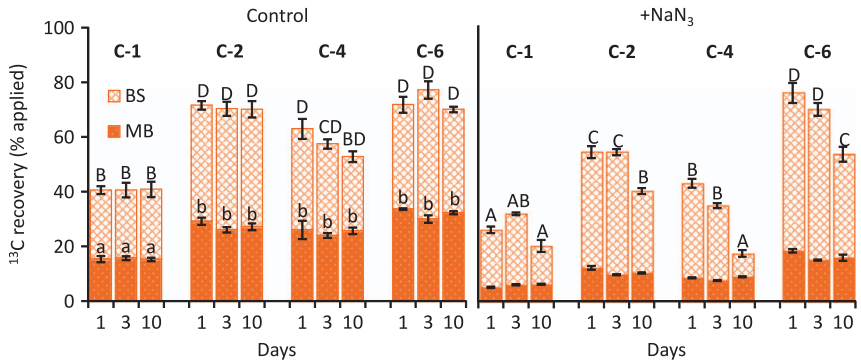

Figure 2 ^{13}C recovery (mean ± s.e.) from various glucose positions in bulk soil and extractable microbial biomass, 1, 3 and 10 days after application in control (left) and azide-exposed soils (right). Significant effects of NaN_3 addition, days and individual glucose positions, according to Tukey Honest Significance Difference (Tukey HSD) *post-hoc* test, in bulk soil (BS) are indicated by upper case letters above the error bars, while extractable microbial biomass (MB) by lower case letters.

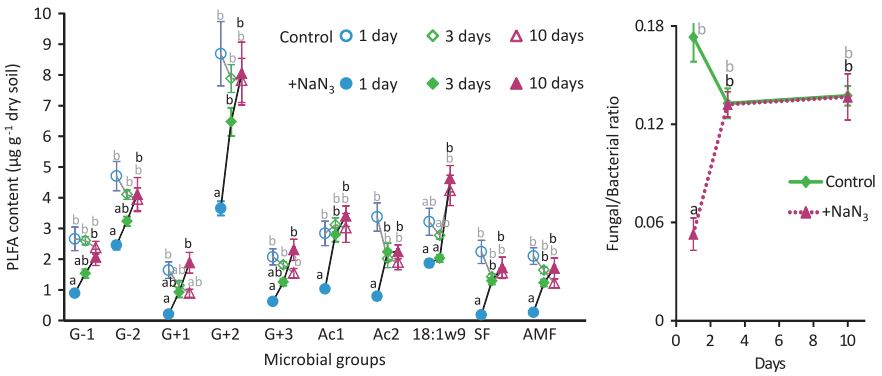

Figure 3 Absolute PLFA contents (mean ± s.e.) of microbial groups (µg g^{-1} dry soil), grouped according to a factor analysis (factor loading see Supplementary Table S2) in control (open markers) and azide-exposed (solid markers) (left) and fungal/bacterial ratios (mean ± s.e.) (right). The letters indicate significant differences ($P<0.05$) between incubation time (within microbial groups' fatty acid content) and the effect of NaN_3 addition. Meaning of microbial group acronyms are: G-1 = Gram negative 1, G-2 = Gram negative 2, G+1 = Gram positive 1, G +2 = Gram positive 2, G+3 = Gram positive 3, Ac1 = Actinomycets 1, Ac2 = Actinomycetes 2, 18:1w9 = fatty acid not associated with any microbial group, SF = saprophytic fungi and AMF = arbuscular micorrhizal fungi.

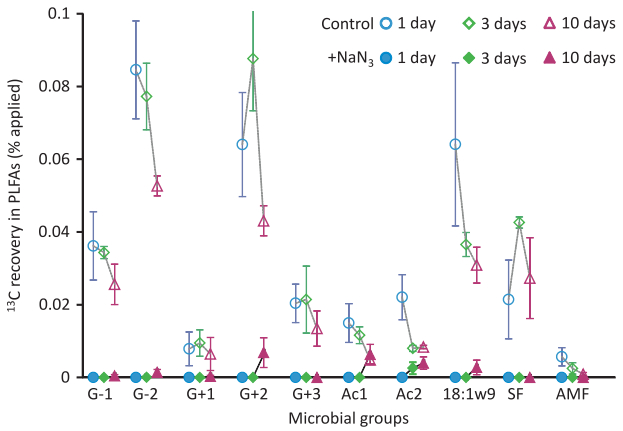

Figure 4 ^{13}C recovery (mean ± s.e.) from applied uniformly labeled ^{13}C glucose in PLFAs of microbial groups in control (open markers) and azide-exposed (solid markers). Meaning of microbial group acronyms are: G-1 = Gram negative 1, G-2 = Gram negative 2, G+1 = Gram positive 1, G+2 = Gram positive 2, G+3 = Gram positive 3, Ac1 = Actinomycets 1, Ac2 = Actinomycetes 2, 18:1w9 = fatty acid not associated with any microbial group, SF = saprophytic fungi and AMF = arbuscular micorrhizal fungi.

addition despite an increase in their fatty acid content (Figure 3, left), revealing dependence on other C sources for their growth.

Discussion

Total CO_2 efflux and glucose mineralization

CO_2 is persistently released from soil exposed to respiration-inhibiting toxicants (for example, NaN_3) or heavy metals inhibiting respiration (for example, cadmium (Cd), mercury (Hg) and copper (Cu); Ausmus *et al.*, 1978; Rozycki and Bartha, 1981; Fliessbach *et al.*, 1994; Trevors, 1996). Application of ^{13}C glucose to NaN_3-inhibited and control soils resulted in high ^{13}C recovery in CO_2 within the first 3 days (Figure 1, bottom), consistent with intense glucose mineralization. Lower ^{13}C recoveries thereafter reflect mineralization of glucose-derived metabolites after exhaustion of glucose (Blagodatskaya *et al.*, 2011). The ^{13}C recovery pattern in CO_2 was similar (C-1 > C-4 > C-2 > C-6) under both conditions. The high ^{13}C recovery from glucose C-1 position in CO_2 reveals that glucose was predominantly catabolized via the pentose phosphate pathway (Caspi *et al.*, 2008; Dijkstra *et al.*, 2011b; Apostel *et al.*, 2015).

Average ^{13}C recovery in CO_2 was 12% higher from inhibited soil compared with control. In contrast, total CO_2 from inhibited soil was half emitted from control (Figure 1, top left). High CO_2 release with low ^{13}C content from control points towards a priming effect, that is, a glucose-induced acceleration of SOM decomposition (Kuzyakov, 2010; Blagodatskaya and Kuzyakov, 2013). Increased ^{13}C recovery and reduced total CO_2 after NaN_3 inhibition could not be explained by a shift towards fermentative metabolism resulting from respiration inhibition, as $^{13}CO_2$ from fermentation would be C-4 dominated instead of C-1. High CO_2 emission from soils with minimized microbial activity can be attributed to release of active oxidative extracellular enzymes (EXOMET) from dead organisms (Maire *et al.*, 2013). To prove or reject the relevance of EXOMET compared with cellular metabolism, investigation of intracellularly formed metabolites (that is, *de novo* formed microbial biomass) was conducted.

^{13}C incorporation into microbial biomass and bulk soil

Glucose is utilized by microorganisms for biosynthesis of various cellular building blocks and as an energy source (Gunina *et al.*, 2014). Recovery of glucose-derived ^{13}C in microbial biomass is indicative of active intracellular biosynthetic processes. ^{13}C recovery in microbial biomass from C-6, C-4 and C-2 was higher than C-1 in control soil (Figure 2, left), with a similar pattern arising in control bulk soil, confirming that microbial products, and not untransformed glucose, are the predominant source of extracellular ^{13}C. The position-specific ^{13}C recovery pattern in bulk soil and microbial biomass complemented the metabolic fluxes observed in CO_2 and confirm that glucose was predominantly metabolized via the pentose phosphate pathway. The dominance of this pathway at 5 °C under moderate C supply reflects the classical metabolic C allocation observed in previous studies (Dijkstra *et al.*, 2011b). Temperature decrease shifts metabolic activity from glycolysis and NADH production to the pentose phosphate pathway and NADPH production in microbial cultures (Wittmann *et al.*, 2007) to meet the pentose and NADPH demands for biosynthesis (Fuhrer and Sauer, 2009). High ^{13}C recovery from positions C-6, C-4 and C-2 implies that, after loss of the C-1, the remaining part of the molecule was allocated to biosynthesis (Gunina *et al.*, 2014). Levels of ^{13}C in microbial biomass did not change between the days in control soils, suggesting that glucose was consumed within the first day and was incorporated into C pools with slower turnover.

In inhibited soil, glucose ^{13}C recovery from C-6 and C-2 in bulk soil and microbial biomass was higher than of C-1 and C-4 (Figure 2, right), suggesting intracellular transformation to pyruvate via the pentose phosphate pathway (Dijkstra *et al.*, 2015) followed by oxidization for energy production. Increased glucose oxidation after pyruvate formation also accounts for the altered pattern of ^{13}C recovery observed in bulk soil, with even stronger decrease in C-4 and C-2 incorporation at day 1 compared with control soil (Dijkstra *et al.*, 2015). Intracellular transformation of glucose after NaN_3 inhibition opposes the concept of extracellular oxidative metabolism (Maire *et al.*, 2013), as surviving microbes must be responsible for the observed transformation. The ≈3-fold lower ^{13}C recovery in microbial biomass and higher recovery in CO_2 following inhibition compared with control

conditions (Figure 1 and 2, bottom) imply that the surviving microbes utilized substantial amount of glucose for energy production. This shift towards energy production may represent an adaptation mechanism by tolerant bacterial strains to overcome inhibition, as microorganisms that survive heavy metal intoxication also divert a large amount of energy from added substrate towards energy-intensive physiological detoxification mechanisms (Gordon *et al.*, 1993). Resistance to toxicants shifts microbial community structure to compensate for the loss of more sensitive populations (Giller *et al.*, 1998). Furthermore, resistance of some Trichoderma strains to NaN_3 was reported by Kelley and Rodriguez-Kabana (1981). Therefore, we conducted PLFA analysis to identify those microbial groups that survive inhibition.

^{13}C incorporation into PLFAs

^{13}C was incorporated into PLFAs of each microbial group in control soils with G-2 and G+2 incorporating two times more than other microbial groups (Figure 4). At room temperatures, growth rate of Gram-negative bacteria is dependent upon the concentration of easily available substrate (Treonis *et al.*, 2004). Therefore, they dominate the rhizosphere, where low molecular weight organic substances are present in high concentrations (Gunina *et al.*, 2014; Apostel *et al.*, 2015). In contrast, Gram-positive bacteria are typically abundant in bulk soil and incorporate C from old SOM (Kramer and Gleixner, 2006). Therefore, ^{13}C recovery within the same range in PLFA of G-2 and G+2 in control soils implies that Gram-positive bacteria profited from lower competitiveness of Gram negatives at low temperature (5 °C). The lack of difference in ^{13}C incorporation into PLFAs between the days was similar to results in microbial biomass, confirming complete glucose incorporation within the first day and slow transformation of ^{13}C in microbial products thereafter.

Ten days after inhibition, incorporation of glucose-derived ^{13}C into fatty acids was only observed in G+2 and actinomycetes (Figure 4), that is, groups known to use old SOM or microbial necromass (McCarthy and Williams, 1992; Kramer and Gleixner, 2006). Therefore, their ^{13}C incorporated into PLFA is likely to occur by recycling of glucose-derived excretion products and not intact glucose. Such recycling of extracellular glucose-derived metabolites explains the decrease in ^{13}C recovery by over 12% in bulk soil 10 days after inhibition. There was no detectable glucose ^{13}C incorporation in any PLFA 3 days after inhibition (Figure 4), despite more than 9% recovery in microbial biomass, suggesting either (1) absence of growth and membrane repair or (2) glucose C was not allocated to fatty acid biosynthesis. To determine the most likely scenario, we examined the fatty acid content of microbial biomass to determine the growth status of the microbial populations.

Effects of NaN_3 on microbial community structure

Comparing the fungal/bacterial ratio in inhibited and control soils at day 1 demonstrated a greater short-term susceptibility of fungi to azide inhibition (Figure 3, right). However, a twofold increase of the fungi/bacteria ratio to a level equal to control soils within 3 days shows fast recovery of fungal biomass.

The fatty acid contents associated with each microbial group were more than twofold lower after inhibition compared with control soil at day 1, likely resulting from cell asphyxiation (Winter *et al.*, 2012). However, the twofold increase in fatty acid content associated with each microbial group in inhibited soils between day 1 and 10 implies that there was growth of the affected microbial groups. This contradicts previous assumptions that microorganisms stressed by exposure to toxicants divert energy from growth to maintenance (Killham, 1985). Furthermore, the increasing fatty acid contents raise the question how microorganisms grow without incorporating glucose into their PLFA. Living microorganisms can utilize microbial necromass from soil (Dippold and Kuzyakov, 2016; Figure 5), whose pool was likely substantial resulting from the death of a high percentage of microorganisms after inhibition. The energy for transforming or recycling of such compounds was provided by an increase in glucose oxidation, which was proven by the 12% increased ^{13}C recovery in CO_2 and the ≈3-fold lower ^{13}C recovery in microbial biomass after inhibition compared with control. Preferential recycling of the cost-intensive alkyl chains of PLFA and other cost-intensive biomass compounds occur under such conditions. This recycling is accompanied by de-novo formation of other cheaper biomass compounds. Therefore, ecosystems are self-regulating systems that evolve mechanisms of self-repair and their biological populations are adapted to resist and recover from environmental fluctuations (EFSA, 2016). Diminishing effects of inhibition over time leads to potential recovery of the microbial groups (EFSA, 2016) as indicated by increase in PLFA content.

Adaptation mechanisms to respiration inhibition

Azide inhibits electron transfer in non-phosphorylating submitochondrial particles at cytochrome oxidase and catalase (Keilin, 1936) resulting in cell asphyxiation (Winter *et al.*, 2012). Continued respiration after inhibition, with intensive intracellular transformation via the pentose phosphate pathway raises the question: How do microorganisms manage intracellular respiration without electron acceptors (NAD^+ or $NADP^+$), which cannot be regenerated after azide inhibition? A common response of bacteria to electron–acceptor limitation is to produce electrically conductive pilus-like appendages called bacterial nanowires (Reguera *et al.*, 2005; Gorby *et al.*, 2006), which anchor between the periplasmic and outer membranes and

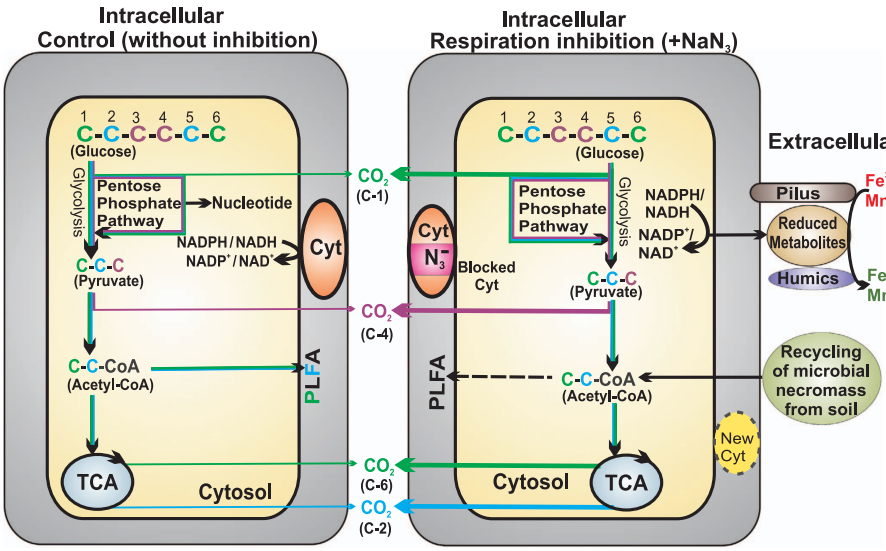

Figure 5 Microbial glucose transformation pathways in control (left) and mechanisms adapted to overcome inhibition (right). Colored arrows correspond to glucose C positions and indicate their fate. The thickness of the colored arrows towards CO_2 is proportional to amount. Black straight and broken arrows indicate metabolites formed or recycled. Black curvy arrows indicate redox processes.

allow transfer of electrons from the cell to minerals containing Fe^{3+} and Mn^{4+} in the extracellular environment (Reguera *et al.*, 2005; Gorby *et al.*, 2006; Figure 5). Other demonstrated mechanisms to overcome inhibition include (1) electron shuttling between the cell and extracellular minerals via humic substances in solution (Lovley *et al.*, 1996; Bi *et al.*, 2013; Piepenbrock *et al.*, 2014) and solid state (Roden *et al.*, 2010) or (2) excretion of reduced metabolites by microorganisms, including quinones (Newman and Kolter, 2000) and phenolic compounds (Vempati *et al.*, 1995; Pentrakova *et al.*, 2013), that transfer electrons to the extracellular environment (Figure 5). Processes outlined above demonstrate that electron transport chain inhibition does not stop intracellular microbial metabolism in soil. Without compound-specific ^{13}C measurement of the extracellular metabolite pool, it is not possible to point out which of these processes for extracellular electron disposal dominated after NaN_3 addition. However, extracellular electron transfer by excretion of reduced metabolites explains the high ^{13}C recovery in the bulk soil compared with microbial biomass during the first 3 days following inhibition. The effectiveness of NaN_3 as a bacteriostat in liquid samples such as antibodies, milk (Winter *et al.*, 2012) or water samples does not contradict our findings, because such samples lack humic substances or minerals (Fe^{3+} and Mn^{4+}) permitting extracellular electron transfer via the above-mentioned mechanisms.

Previously, persistent CO_2 release from soil with eliminated or inhibited respiration was attributed to abiotic processes (Rozycki and Bartha, 1981; Trevors, 1996) and extracellular oxidative metabolism (Maire *et al.*, 2013). Our data clearly demonstrate that inhibition of electron transport chain cannot stop intracellular glucose metabolism: microorganisms circumvent respiration inhibition via temporary extracellular electron transfer, giving organisms a chance to reconstruct new electron transport chains and resume normal (aerobic) respiration. Thus, even under respiration inhibition no indication for extracellular glucose metabolism could be perceived. The ability of microorganisms to overcome limitations of intracellular metabolism by utilizing SOM resources is important for understanding the origin of CO_2 emitted from soils with respiration-inhibiting toxicants (Bond *et al.*, 1976; Ausmus *et al.*, 1978; Trevors, 1996). Heavy metals such as Cd, Hg and Cu, which are widespread in the environment due to their industrial, agricultural, medical and technological application, inhibit respiration (Belyaeva *et al.*, 2012). However, their presence in organic or clayey soils does not stop respiration (Bond *et al.*, 1976; Ausmus *et al.*, 1978; Fliessbach *et al.*, 1994), a phenomenon that could similarly be explained by extracellular electron transfer because such soils are rich in humic substances and minerals (Fe^{3+} and Mn^{4+}) functioning as extracellular electron acceptors. Microorganisms' tolerance and resistance to copper-based fungicides could also be attributed to extracellular electron transfer. Therefore, the mechanisms proven from metabolic perspective in this study contribute to a better understanding of microbial resilience and resistance to direct respiration-inhibiting toxicants (for example, azides, cyanides), pesticides (for example, phosphides and phosphines) or heavy metals (for example, Cu and Hg) and subsequent ecological recovery after perturbation. Such mechanisms are limited to portion of microorganisms activated by glucose (Monard *et al.*, 2008) and toxicants that inhibit respiratory chains directly.

Conclusions

Combining position-specific ^{13}C labeling with compound-specific ^{13}C-PLFA analysis proved to be a valuable tool to understand how microorganisms overcome respiration inhibition. Glucose was metabolized by soil microorganisms via the pentose phosphate pathway irrespective of respiration inhibition. NaN_3 reduced total CO_2 efflux twofold but increased ^{13}C recovery in released CO_2 by 12% compared with control soils. The low ^{13}C recovery in microbial biomass increased pyruvate oxidation and increased proportion of glucose-derived metabolites in extracellular microbial products following NaN_3 application provide evidence for increased glucose use for energy production and synthesis of extracellular electron transport compounds to bypass inhibition. Resources for growth were recycled from the large pool of microbial necromass resulting from toxicant addition. Consequently, to overcome intracellular inhibition of the electron transport chain, microorganisms most likely coupled intracellular metabolism with extracellular redox processes. This is possible only in soil and similar environments rich in electron acceptors. Construction of new electron transport chains and resumption of aerobic respiration as well as recovery of microbial groups occurred within 10 days at 5 °C. We assume this bypass of respiration inhibition will be much faster at high temperatures.

These results suggest that the persistent CO_2 efflux after azide addition to soil is as a result of intracellular oxidation of SOM followed by extracellular electron disposal. This mechanism is also likely to account for microbial tolerance to, for example, heavy metals and other toxicants directly altering microbial respiration in soils but requires confirmation by extending this position-specific labeling approach on soils contaminated with a broad spectrum of toxicants. Finally, this metabolic tracing approach provides an understanding of the impacts of chemicals such as azides, cyanides and heavy metals on soil C cycling following contamination and enables development of unique insights concerning soil-specific microbial mechanisms to overcome respiration inhibition.

Conflict of Interest

The authors declare no conflict of interest.

Acknowledgements

We thank the DFG for funding (DI-2136/1-1 and NTS 186/1006-1/P) and DAAD for funding Ezekiel Bore. We thank the technical staff of Goettingen University, in particular Karin Schmidt and Anita Kriegel, for microbial biomass C content determination, the entire team at KOSI (Centre for Stable Isotopes Analysis) for $\delta^{13}C$ analysis and Joshua Bostic for English proofreading.

References

Apostel C, Dippold M, Glaser B, Kuzyakov Y. (2013). Biochemical pathways of amino acids in soil: assessment by position-specific labeling and 13C-PLFA analysis. *Soil Biol Biochem* **67**: 31–40.

Apostel C, Dippold M, Kuzyakov Y. (2015). Biochemistry of hexose and pentose transformations in soil analyzed by position-specific labeling and 13C-PLFA. *Soil Biol Biochem* **80**: 199–208.

Ausmus BS, Dodson GJ, Jackson DR. (1978). Behavior of heavy-metal in forest microcosms. 3. Effects on litter-carbon metabolism. *Water Air Soil Pollut* **10**: 19–26.

Babich H, Stotzky G. (1985). Heavy metal toxicity to microbe-mediated ecologic processes: a review and potential application to regulatory policies. *Environ Res* **36**: 111–137.

Belyaeva EA, Sokolova TV, Emelyanova LV, Zakharova IO. (2012). Mitochondrial electron transport chain in heavy metal-induced neurotoxicity: effects of cadmium, mercury, and copper. *Sci World J* **2012**: 136063–136063.

Bi R, Lu Q, Yu W, Yuan Y, Zhou S. (2013). Electron transfer capacity of soil dissolved organic matter and its potential impact on soil respiration. *J Soil Sediment* **13**: 1553–1560.

Blagodatskaya E, Kuzyakov Y. (2013). Active microorganisms in soil: critical review of estimation criteria and approaches. *Soil Biol Biochem* **67**: 192–211.

Blagodatskaya E, Yuyukina T, Blagodatsky S, Kuzyakov Y. (2011). Three-source-partitioning of microbial biomass and of CO2 efflux from soil to evaluate mechanisms of priming effects. *Soil Biol Biochem* **43**: 778–786.

Blankinship JC, Becerra CA, Schaeffer SM, Schimel JP. (2014). Separating cellular metabolism from exoenzyme activity in soil organic matter decomposition. *Soil Biol Biochem* **71**: 68–75.

Bond H, Lighthart B, Shimabuku R, Russell L. (1976). Some effects of cadmium on coniferous forest soil and litter microcosms. *Soil Sci* **121**: 278–287.

Bremer E, van Kessel C. (1990). Extractability of microbial ^{14}C and ^{15}N following addition of variable rates of labelled glucose and $(NH_4)_2SO_4$ to soil. *Soil Biol Biochem* **22**: 707–713.

Caspi R, Foerster H, Fulcher CA, Kaipa P, Krummenacker M, Latendresse M *et al.* (2008). The MetaCyc database of metabolic pathways and enzymes and the BioCyc collection of Pathway/Genome Databases. *Nucleic Acids Res* **36**: D623–D631.

Dijkstra P, Dalder JJ, Selmants PC, Hart SC, Koch GW, Schwartz E *et al.* (2011a). Modeling soil metabolic processes using isotopologue pairs of position-specific C-13-labeled glucose and pyruvate. *Soil Biol Biochem* **43**: 1848–1857.

Dijkstra P, Salpas E, Fairbanks D, Miller EB, Hagerty SB, van Groenigen KJ *et al.* (2015). High carbon use efficiency in soil microbial communities is related to balanced growth, not storage compound synthesis. *Soil Biol Biochem* **89**: 35–43.

Dijkstra P, Thomas SC, Heinrich PL, Koch GW, Schwartz E, Hungate BA. (2011b). Effect of temperature on metabolic activity of intact microbial communities: evidence for altered metabolic pathway activity but not for increased maintenance respiration and reduced carbon use efficiency. *Soil Biol Biochem* **43**: 2023–2031.

Dippold M, Biryukov M, Kuzyakov Y. (2014). Sorption affects amino acid pathways in soil: implications from position-specific labeling of alanine. *Soil Biol Biochem* **72**: 180–192.

Dippold MA, Kuzyakov Y. (2013). Biogeochemical transformations of amino acids in soil assessed by position-specific labelling. *Plant Soil* **373**: 385–401.

Dippold MA, Kuzyakov Y. (2016). Direct incorporation of fatty acids into microbial phospholipids in soils: position-specific labeling tells the story. *Geochim Cosmochim Acta* **174**: 211–221.

EFSA. (2016). Recovery in environmental risk assessments at EFSA. *EFSA J* **14**: 4313.

Fischer H, Ingwersen J, Kuzyakov Y. (2010). Microbial uptake of low-molecular-weight organic substances out-competes sorption in soil. *Eur J Soil Sci* **61**: 504–513.

Fischer H, Meyer A, Fischer K, Kuzyakov Y. (2007). Carbohydrate and amino acid composition of dissolved organic matter leached from soil. *Soil Biol Biochem* **39**: 2926–2935.

Fliessbach A, Martens R, Reber HH. (1994). Soil microbial biomass and microbial activity in soils treated with heavy metal contaminated sewage sludge. *Soil Biol Biochem* **26**: 1201–1205.

Frostegård Å, Tunlid A, Bååth E. (1991). Microbial biomass measured as total lipid phosphate in soils of different organic content. *J Microbiol Methods* **14**: 151–163.

Fuhrer T, Sauer U. (2009). Different biochemical mechanisms ensure network-wide balancing of reducing equivalents in microbial metabolism. *J Bacteriol* **191**: 2112–2121.

Gearing JN. (1991). The study of diet and trophic relationships through natural abundance ^{13}C. In: Coleman DC, Fry B (eds). *Carbon Isotope Techniques.* Academic Press: New York, pp 201–218.

Giller KE, Witter E, McGrath SP. (1998). Toxicity of heavy metals to microorganisms and microbial processes in agricultural soils: a review. *Soil Biol Biochem* **30**: 1389–1414.

Glaser B, Amelung W. (2002). Determination of C-13 natural abundance of amino acid enantiomers in soil: methodological considerations and first results. *Rapid Commun Mass Spectrom* **16**: 891–898.

Gorby YA, Yanina S, McLean JS, Rosso KM, Moyles D, Dohnalkova A *et al.* (2006). Electrically conductive bacterial nanowires produced by Shewanella oneidensis strain MR-1 and other microorganisms. *Proc Natl Acad Sci USA* **103**: 11358–11363.

Gordon AS, Harwood VJ, Sayyar S. (1993). Growth, copper-tolerant cells, and extracellular protein production in copper-stressed chemostat cultures of *Vibrio alginolyticus*. *Appl Environ Microbiol* **59**: 60–66.

Gunina A, Dippold MA, Glaser B, Kuzyakov Y. (2014). Fate of low molecular weight organic substances in an arable soil: from microbial uptake to utilisation and stabilisation. *Soil Biol Biochem* **77**: 304–313.

Gunina A, Kuzyakov Y. (2015). Sugars in soil and sweets for microorganisms: review of origin, content, composition and fate. *Soil Biol Biochem* **90**: 87–100.

ISO 16072. (2002). *Soil quality—Laboratory Methods for Determination of Microbial Soil Respiration*. International Organization for Standardization: Geneva, Switzerland.

Keilin D. (1936). The action of sodium azide on cellular respiration and on some catalytic oxidation reactions. *Proc Roy Soc Lond B Biol Sci* **121**: 165–173.

Kelley WD, Rodriguez-Kabana R. (1981). Effects of annual applications of sodium azide on soil fungal populations with emphasis on Trichoderma species. *Pestic Sci* **12**: 235–244.

Killham K. (1985). A physiological determination of the impact of environmental stress on microbial bomass. *Environ Pollut A* **38**: 283–294.

Kramer C, Gleixner G. (2006). Variable use of plant- and soil-derived carbon by microorganisms in agricultural soils. *Soil Biol Biochem* **38**: 3267–3278.

Kuzyakov Y. (2010). Priming effects: interactions between living and dead organic matter. *Soil Biol Biochem* **42**: 1363–1371.

Lovley DR, Coates JD, BluntHarris EL, Phillips EJP, Woodward JC. (1996). Humic substances as electron acceptors for microbial respiration. *Nature* **382**: 445–448.

Maire V, Alvarez G, Colombet J, Comby A, Despinasse R, Dubreucq E *et al.* (2013). An unknown oxidative metabolism substantially contributes to soil CO_2 emissions. *Biogeosciences* **10**: 1155–1167.

Mau RL, Liu CM, Aziz M, Schwartz E, Dijkstra P, Marks JC *et al.* (2015). Linking soil bacterial biodiversity and soil carbon stability. *ISME J* **9**: 1477–1480.

McCarthy AJ, Williams ST. (1992). Actinomycetes as agents of biodegradation in the environment—a review. *Gene* **115**: 189–192.

Monard C, Binet F, Vandenkoornhuyse P. (2008). Short-term response of soil bacteria to carbon enrichment in different soil microsites. *Appl Environ Microbiol* **74**: 5589–5592.

Newman DK, Kolter R. (2000). A role for excreted quinones in extracellular electron transfer. *Nature* **405**: 94–97.

Pentrakova L, Su K, Pentrak M, Stuck JW. (2013). A review of microbial redox interactions with structural Fe in clay minerals. *Clay Miner* **48**: 543–560.

Piepenbrock A, Schroeder C, Kappler A. (2014). Electron transfer from humic substances to biogenic and abiogenic Fe(III) oxyhydroxide minerals. *Environ Sci Technol* **48**: 1656–1664.

Reguera G, McCarthy KD, Mehta T, Nicoll JS, Tuominen MT, Lovley DR. (2005). Extracellular electron transfer via microbial nanowires. *Nature* **435**: 1098–1101.

Roden EE, Kappler A, Bauer I, Jiang J, Paul A, Stoesser R *et al.* (2010). Extracellular electron transfer through microbial reduction of solid-phase humic substances. *Nat Geosci* **3**: 417–421.

Rozycki M, Bartha R. (1981). Problems associated with the use of azide as an inhibitor of microbial activity in soil. *Appl Environ Microbiol* **41**: 833–836.

Scandellari F, Hobbie EA, Ouimette AP, Stucker VK. (2009). Tracing metabolic pathways of lipid biosynthesis in ectomycorrhizal fungi from position-specific ^{13}C-labelling in glucose. *Environ Microbiol* **11**: 3087–3095.

Schimel J. (2013). Soil carbon microbes and global carbon. *Nat Climate Change* **3**: 867–868.

Schmitt J, Glaser B, Zech W. (2003). Amount-dependent isotopic fractionation during compound-specific isotope analysis. *Rapid Commun Mass Spectrom* **17**: 970–977.

Treonis AM, Ostle NJ, Stott AW, Primrose R, Grayston SJ, Ineson P. (2004). Identification of groups of metabolically-active rhizosphere microorganisms by stable isotope probing of PLFAs. *Soil Biol Biochem* **36**: 533–537.

Trevors JT. (1996). Sterilization and inhibition of microbial activity in soil. *J Microbiol Methods* **26**: 53–59.

Vempati RK, Kollipara KP, Stucki JW, Wilkinson H. (1995). Reduction of structural iron in selected iron-bearing minerals by soybean root exudates grown in an in-vitro geoponicsystem. *J Plant Nutr* **18**: 343–353.

Voroney RP, Paul EA. (1984). Determination of KC and KN insitu for calibration of the chloroform fumigation incubation method. *Soil Biol Biochem* **16**: 9–14.

Winter C, Kerros M-E, Weinbauer MG. (2012). Effects of sodium azide on the abundance of prokaryotes and viruses in marine samples. *PLoS One* **7**: e37597.

Wittmann C, Weber J, Betiku E, Kroemer J, Boehm D, Rinas U. (2007). Response of fluxome and metabolome to temperature-induced recombinant protein synthesis in Escherichia coli. *J Biotechnol* **132**: 375–384.

Wu J, Joergensen RG, Pommerening B, Chaussod R, Brookes PC. (1990). Measurement of soil microbial biomass C by fumigation extraction—an automated procedure. *Soil Biol Biochem* **22**: 1167–1169.

Zelles L. (1999). Fatty acid patterns of phospholipids and lipopolysaccharides in the characterisation of microbial communities in soil: a review. *Biol Fertil Soils* **29**: 111–129.

Zelles L, Bai QY, Rackwitz R, Chadwick D, Beese F. (1995). Determination of phospholipid-derived and lipopolysaccharide-derived fatty-acids as an estimate of microbial biomass and community structures in soils. *Biol Fertil Soils* **19**: 115–123.

Supplementary Information accompanies this paper on The ISME Journal website (http://www.nature.com/ismej)